Strategies for Selecting Potentially Effective Biofumigant Species for Optimal Biofumigation Outcomes

Juan Manuel Arroyo , Jose Soler , Rubén Linares , Daniel Palmero *

Posted Date: 5 November 2024

doi: 10.20944/preprints202411.0247.v1

Keywords: Biofumigation; Glucosinolates (GSL); Brassicaceae species; Soil-Borne Diseases

Article

Strategies for Selecting Potentially Effective Biofumigant Species for Optimal Biofumigation Outcomes

Juan Manuel Arroyo [1], Jose Soler [1], Rubén Linares [1] and Daniel Palmero [1,*]

[1] Departmento de Producción Agraria, Escuela Técnica Superior de Ingeniería Agronómica, Alimentaria y de Biosistemas, Universidad Politécnica de Madrid, Avenida Puerta de Hierro, 4, 28040 Madrid, España.

* Correspondence: daniel.palmero@upm.es

Abstract: Soil-borne diseases threaten sustainable agriculture, traditionally managed by chemical fumigants, whose use is now restricted due to environmental and health concerns. This study evaluates the biofumigation potential of *Brassicaceae* species, specifically *Brassica carinata* A.Braun., *Brassica juncea* (L.) Vassiliĭ Matveievitch Czernajew., *Raphanus sativus* L., and *Sinapis alba* L., cultivated in central Spain. Field trials across two growing cycles assessed biomass production, glucosinolates (GSLs) concentration, photosynthetically active radiation (PAR) interception, and radiation use efficiency (RUE). Biomass production varied across species and sampling dates, with *S. alba* and *R. sativus* outperforming other species in shorter cycles, while *B. juncea* and *B. carinata* showed more efficient GLS profile to soil-borne diseases control, particularly in aliphatic GSLs like Sinigrin. Results highlight *B. juncea* and *B. carinata* as potent biofumigants due to their high GSL levels, whereas *S. alba* and *R. sativus* are more suited to early biomass production. The study also explores the Chlorophyll Content Index (SPAD) as a potential field indicator of GSL concentration, providing a practical approach for optimizing biofumigation timing. These findings support the selection of specific Brassicaceae species adapted to climatic conditions and crop cycles for effective biofumigation in sustainable agricultural practices.

Keywords: biofumigation; glucosinolates (GSL); brassicaceae species; soil-borne diseases

1. Introduction

Soil-borne diseases pose a significant threat to sustainable agricultural production, primarily impacting crop yields and quality through infections caused by fungi, bacteria, and nematodes. Traditional control measures often rely on chemical fumigants. However, the negative environmental effects, health hazards, societal concerns, and the development of new environmental strategies, such as the "Farm to Fork Strategy," have heavily restricted the use of these synthetic chemical compounds. This growing concern has spurred the search for sustainable alternatives that may reduce the quantity and toxicity of synthetic chemicals applied to agricultural fields, with biofumigation emerging as a particularly promising strategy [1–3].

The term biofumigation was initially proposed by [4]. Although initially defined as the cultivation of specific plants that naturally produce bioactive compounds with biocidal properties, followed by the incorporation of plant residues into the soil through chopping and rapid mixing [3,5,6], biofumigation now encompasses various application methods. These include cover cropping, whole plant incorporation, and the use of isolated plant products, such as industrially formulated defatted seed meals or concentrated applications of plant essential oils or distilled essences [2,7,8].

While various species and residues have been investigated for biofumigation (e.g., *Allium* spp., *Lavandula* spp., *Sorghum* spp., *Tagetes lucida* Cav, *Azadirachta indica* A.Juss) [9–14], studies have shown that plants of the Brassicaceae family are among the most effective. These plants grow rapidly,

 doi:10.20944/preprints202411.0247.v1

produce large amounts of biomass [15], and some species synthesize high levels of GSLs in their tissues.

Due to their high GSL concentrations, genera such as *Brassica*, *Raphanus*, *Sinapis*, and *Eruca* are the most commonly used for biofumigation [16–19]. GSLs are secondary metabolites found in some plants (e.g., *Brassicaceae*, *Capparidaceae*, *Tropaeolaceae*, *Moringaceae*, and *Amaryllidaceae* families) [6,20]. GSLs are composed of β-thioglucoside N-hydroxysulfates (a common functional group), with a side group (R – a variable aglycone side chain derived from one of eight natural amino acids) and a sulfur-linked β-d-glucopyranose moiety [21]. The R group is retained in the resulting isothiocyanates (ITC), influencing their biocidal activity [22].

The decomposition of brassica tissues and enzymatic hydrolysis of GSLs by myrosinase produce toxic ITC, in addition to other compounds such as thiocyanate, nitriles, organic cyanides, methyl sulfide, dimethyl sulfide, and methanethiol, formed through various chemical reactions. Although these additional compounds are typically less toxic than isothiocyanates, they are often present in large quantities and may also contribute to biofumigation [23–25]. Among these compounds, notably ITC are highly effective for disease control due to their broad-spectrum antimicrobial properties [18–26].

In general, the highest GSL concentrations are found in seeds, followed by above-ground and below-ground tissues [17–28]. GSL concentration in seeds is typically 8-10 times higher than in other parts of the plant [1], although it varies with growth stage, environment, and species interactions [27,29].

High ITC levels are needed for effective soil disinfection through biofumigation. For example, soil sterilization is calculated at effective values of 517 to 1294 μmol/g soil of methyl isothiocyanate [30]. However, lower ITC concentrations in the soil (150 μmol/g soil of ally or 182 μmol/g soil of methyl isothiocyanate) are sufficient to control most soil-borne and diseases, such as *Verticillium dahlia* or larvae of the black vine weevil [31,32]. Thus, although plant GSL concentration is crucial to the success of biofumigation, the key factor is the release of ITCs into the soil [33].

Biofumigation has several potential benefits, not only providing a natural alternative to synthetic fumigants with reduced environmental and human health risks but also offering a diverse array of bioactive chemicals that soil-borne diseases may not be adapted to resist. Biofumigation contributes organic matter to the soil, improving soil structure, enhancing soil health through erosion prevention, increasing nutrient availability, reducing nitrogen leaching, stimulating beneficial or pathogen-suppressive microbial communities, and suppressing weed pressure, potentially reducing costs for growers) [2,22].

As several studies have shown the effectiveness of biofumigation is linked to GLSs tissues concentration but also, in especially with each species ability to biomass accumulation [34,35]. In turn, biomass accumulation ability is influenced by specie ability to intercept and utilize photosynthetically active radiation (PAR), as well as their RUE [15].

This study aims to evaluate biofumigant species suitable for use in extensive horticultural crops in central Spain. Specifically, the research focuses on identifying species that not only possess high levels of bioactive GSLs but also demonstrate effective adaptation to the region's climatic conditions and cultivation cycles. By evaluating these species in terms of biomass production, GSL concentration, and seasonal variations, this study seeks to optimize biofumigation practices that can be integrated into local crop rotation and management systems.

2. Materials and Methods

2.1. Location and Soil and Climatic Conditions

The trial was conducted at the Experimental Fields of ETSIAAB (Polytechnical University of Madrid) during the 2022-2023 and 2023-2024 agricultural growing cycles, hereafter referred to as first and second cycle, respectively. The soil in the experimental plot has a sandy loam texture, with a

 doi:10.20944/preprints202411.0247.v1

basic pH of 7.8 and low organic matter content (1.2%). The carbon/nitrogen (C/N) ratio is 8, and the electrical conductivity (EC) measured in a 1:5 extract is 0.16 dS/m. High levels of calcium (Ca ≥ 2500 mg/kg), magnesium (Mg ≥ 250 mg /kg), potassium (K ≥ 300 mg/kg), and phosphorus (P ≥ 60 mg/kg) were detected, based on analyses carried out on four soil samples, one per trial block, collected from the 0-30 cm and 30-60 cm horizons.

According to the Köppen classification, the climate in the region is temperate with dry or hot summers (Csa), with a mean annual rainfall of 379 mm and a mean annual temperature of 14.6 °C (Castilla-La Mancha, i.e., Toledo, Ciudad Real, Albacete). According to the UNESCO-FAO classification, the specific climate at the trial site (Madrid) is described as a "temperate climate with mild winters, xeric, attenuated thermomediterranean," with an average annual rainfall of 421 mm and an average annual temperature of 15.1 °C.

The weather conditions in 2022 and 2023 in terms of thermal and rainfall patterns were very different: 2022 had a very dry autumn and cold winter with a prolonged frost period, whereas 2023 was characterized by abundant rainfall in autumn and mild winter.

2.2. Experimental Design

The experimental design followed a randomized block layout with four replicates, with the biofumigant species being the main factor. Four species were included: *B. carinata* (cv. Eleven), *B. juncea* (cv. Scala), *R. sativus* (cv. Córdoba), and *S. alba* (cv. Venice). Each elementary plot measured 10 m in length and 3.6 m in width, with a total area of 36 m².

Sowing took place on September 22, 2022, and September 29, 2023, using a 1.2 m wide experimental seeder. Seeding rates were 12.5 kg/ha for *B. carinata* and *B. juncea*, and 25 kg/ha for *R. sativus* and *S. alba*. To promote germination in 2022, two emergency irrigations of 15 mm each were applied at the end of September and early October. In 2023, rainfall during the same period was sufficient to ensure good germination, with nascence rates of 75-80% for all species except *B. juncea*, which exhibited a rate of 32%. Given this low rate, germination and viability tests (tetrazolium test) were conducted, confirming that the low germination was not due to seed quality but to intrinsic characteristics of the species. Mineral fertilization in both growing cycles consisted of the application of 400 kg/ha of a complex N-P-K (S) 15-15-15 (13) fertilizer before sowing.

2.3. Analytical Determinations

In each elementary plot, various parameters were evaluated throughout the growth cycle of the biofumigant species, focusing on biomass production and distribution, as well as the physiological development of the plants. The determinations included:

Biomass Production: Total biomass was quantified, distinguishing between the aboveground part and the roots, at different points during the cycle. For this, a 0.5 m² area (1 m x 0.5 m) from each elementary plot was manually harvested on the following dates: January 23 and March 27, 2023 (123 and 186 days after sowing, respectively), and December 11, 2023, and January 29, 2024 (73 and 122 days after sowing, respectively). After plant extraction, the roots were separated from the aboveground part for all plants, and fresh biomass was measured for both root and aboveground portions. A subsample of three representative plants was then selected, and the dry matter content of the root and aboveground biomass was determined separately after drying in a forced-air oven at 65°C until a constant weight was achieved. By applying the dry matter content of the root and aboveground tissues to their respective fresh biomasses, root (RDB) and aboveground dry biomasses (ADB) were obtained, with the sum of these values representing the total dry biomass (TDB).

GLS extraction, purification, desulfatation, and analysis followed ISO Norm (1992) with some adaptations. In short, 50 mg of ground powder was placed in two 10 mL test tubes, to which 1.5 mL of 70% methanol and 100 µL of glucotropaeolin (5 mM and 20 mM, respectively), as internal standards (reference 89216; PhytoLab GmbH & Co. KG, Vestenbergsgreuth, Germany), were added. The tubes were kept in a water bath at 80 ºC for GLSs extraction. After 20 minutes at room temperature, the tubes were centrifuged at 3600 rpm for 20 minutes, and the supernatants were reserved for analysis.

 doi:10.20944/preprints202411.0247.v1

For GLSs purification, 96-well filter plates loaded with A25 DEAE Sephadex ion-exchange resin were prepared using a Millipore multiscreen column loader. 150 µL of 60% methanol was added to each well. After one hour, the liquid was removed with a vacuum pump. 300 µL of the sample supernatant was transferred to each well, and the liquid was again removed using the vacuum pump. After this, the wells were washed twice with 150 µL of 60% methanol and twice with water.

For enzymatic desulfatation of GLSs, 10 µL of water and 10 µL of sulfatase solution were added to each well, and the plates were kept overnight at room temperature. Desulfoglucosinolates were eluted by washing twice with 100 µL of 60% methanol and twice with water. The resulting collected samples containing desulfoglucosinolates were stored at −20 ºC until analysis by HPLC.

The HPLC system consisted of a Waters 1525 binary pump, a Waters 2489 UV/visible detector set at 229 nm, and a Waters 2707 Autosampler (Waters Corporation, Milford, MA, USA). The column used was a Kinetex C18 of 250 x 4.6 mm, 100 Å ID, with a particle size of 5 µm (Phenomenex, Torrance, CA, USA). HPLC analysis was performed using water (solvent A) and 20% acetonitrile (solvent B) as eluents, with the following gradient: 2 minutes of solvent B at 0%, 23 minutes increasing solvent B to 100%, 5 minutes reducing solvent B back to 0%, and 5 minutes maintaining solvent B at 0%, at a flow rate of 1 mL/min and an oven temperature of 40 °C. Water quality was maintained at 18.2-megohm Milli-Q Direct Water (Merck Millipore, Darmstadt, Germany) for all analytical steps. Quantification of desulfoglucosinolates was done using response factors previously reported by ISO Norm (1992) and Yi et al. (2016) for GLSs not included in the ISO Norm. The GLSs analyzed are shown in Table 1.

Table 1. Nature and characteristics of the glucosinolates analyzed in the biomass of the biofumigant species (Adapted by [21,35]).

Type Trivial name	Chemical name	Main Hydrolysis Product
Aliphatic		
Epiprogoitrin	2(S)-Hydroxy-3-butenylglucosinolate	Oxazolidine-2-thiones
Glucoalyssin	5-Methylsulphinylpentyl	Isothiocyanate
Glucobrassicanapin	4-Pentenyl	Isothiocyanate
Glucoerucin	4-Methylthiobutyl	Isothiocyanate (Erucin)
Glucoiberverin	3-Methylthiopropyl	Isothiocyanate
Gluconapin	3-Butenyl	Isothiocyanate
Glucoraphanin	4-Methylsulphinylbutyl	Isothiocyanate (Sulforaphane)
Glucoraphasatin	4-Methylsulfanyl-3-butenyl	Isothiocyanate
Napoleiferin	5-Allyl-1,3-oxazolidin-2-thione	Isothiocyanate
Progoitrin	2-Hydroxy-3-butenyl	Oxazolidine-2-thiones
Sinigrin	2-Propenyl	Isothiocyanate (Allyl)
Aromatic		
Gluconasturtiin	2-Phenylethyl	Isothiocyanate (Phenethyl)
Glucotropaeolin	Benzyl	Isothiocyanate (Benzyl)
Sinalbin	4-hydroxybenzyl glucosinolate;	Nitrile
Indolyl		
4-Hydroxyglucobrassicin	4-Hydroxy-3-indolylmethyl	Thiocyanate
Glucobrassicin	3-Indolylmethyl	Indolyl-3-carbinol

The fraction of Photosynthetically Active Radiation (PAR) intercepted by the canopy (fIPAR) was calculated as the ratio between intercepted PAR (incident PAR – transmitted PAR) and incident PAR, measured at solar noon on each sampling date, always under clear sky conditions. Based on the fIPAR values, the calculation of PAR intercepted by the crop from sowing to each biomass sampling date was divided into as many sub-periods as there were fIPAR measurements. The intercepted PAR value for each sub-period was calculated by multiplying the incident PAR for that

 doi:10.20944/preprints202411.0247.v1

sub-period (daily incident PAR data obtained from the meteorological station located near the trial site) by the arithmetic mean of the fIPAR values determined at the beginning and end of that sub-period.

In turn, the RUE was calculated as an average RUE value for the period between the sowing date and each of the two biomass sampling dates for the biofumigant species. This was determined as the ratio between the TDB, in g of dry matter/m², and the amount of PAR intercepted by the canopy, in MJ/m², during the same time period. Thus, RUE, in g of dry matter/MJ, expresses the efficiency of the plant in converting intercepted radiation into biomass.

Chlorophyll content in the leaves of the biofumigant species was measured using a SPAD meter at different points in the growth cycle as an indicator of the plant's nutritional status. On each sampling date, 15 measurements were taken in each elementary plot (one leaf per plant from 15 plants).

Table 2 provides information on the procedures and equipment used to carry out the analytical determinations in 2022 and 2023, respectively.

Table 2. Parameters and Determinations Carried Out in the Biofumigant Species Trial.

Parameter	Measurement dates 2022/23 (das *)	Measurement dates 2023/24 (das)	Equipment	Method/procedure
Fraction of intercepted PAR (fIPAR)	22, 41, 67, 110, 123, 137, 161, 186		LI-191-R Quantum line sensor	fIPAR = [Incident PAR - Transmitted PAR] / Incident PAR Transmitted PAR: average value of 3 measurements per elementary plot
SPAD	49, 70, 114, 138, 160, 174, 186.	122	SPAD-502® chlorophyll meter (Konica Minolta Inc., Japan)	Average value of 15 measurements (one leaf from 15 plants) per elementary plot and measurement date
Biomass produced: total, root, and aerial part	123 ,186	73 ,122	Precision balances and drying oven	Sampled area per elementary plot: 0.5 m² (1 m x 0.5 m)
Glucosinolate concentration and types in the aerial part	123, 186	120, 190	Lyophilizer (Lyoquest 55 plus-Telstar), IKA A11 basic analytical mill (IKA-Werke GmbH & Co. KG)	Leaf or root samples were frozen shortly after collection at -80 °C. The samples were lyophilized and maintained in a drying oven at 80 ºC for 24 h for myrosinase inactivation, then ground.

(*): Days after sowing date. Emergence (50% germination rate) occurred approximately 9 days after sowing.

2.4. Statistical Analysis

An analysis of variance on the Biomass, fIPAR, RUE, SPAD, GSLs concentration were performed using Fisher's least significant difference (LSD) tests at 95.0% confidence. The tests were carried out using STATGRAPHICS Centurion XVIII statistical package software (StatPoint, Inc., Herndon, VA, USA). In order to estimate the correlation between the different parameters evaluated, the simple regression analysis was adjusted to the non-linear inverse-X model as it showed the highest R^2 value.

 doi:10.20944/preprints202411.0247.v1

3. Results

3.1. Agronomic Performance and Biomass Production

The field trial was repeated over two consecutive growing cycles, and in both cycles, significant differences were detected in the biomass produced by the biofumigant species analyzed. These differences and sampling variations were dependent on the growing cycle and the timing of the sampling (Table 3).

Table 3. Values and statistical analysis of Total Dry Biomass (TDB) production parameters and its components (Aboveground Dry Biomass - ADB and Root Dry Biomass - RDB) for the biofumigant species in the two analyzed growing cycles.

Growing cycle	**1st cycle (2022-23)**						**2nd cycle (2023/24)**					
Sampling date	***23-01-23 (123 das)***			***27-03-23 (186 das)***			***11-12-23 (73 das)***			***29-01-24 (122 das)***		
Specie	**ADB[1]**	**RDB**	**TDB**	**ADB**	**RDB**	**TDB**	**ADB**	**RDB**	**TDB**	**ADB**	**RDB[1]**	**TDB**
B. carinata	763,9	73,1	837	576,4 ab	39,9 c	616,3 ab	315,0 b	73,1 c	388,1 b	515,6	85,3 b	600,9
B. juncea	642,5	124,8	767,3	735,3 a	92,1 ab	827,5 a	130,1 c	31,3 d	161,5 c	383,8	148,4 b	532,2
R. sativus	641,6	122	763,6	598,9 ab	131,4 a	730,3 ab	380,4 b	202,0 a	582,4 a	354,1	238,5 a	592,6
S. alba	647,2	67,4	714,7	493,5 b	56,5 bc	550,1 b	507,3 a	143,4 b	650,7 a	605	83,7 b	688,7
p value	ns[2]	ns	ns	*	**	*	***	***	***	n.s.	**	n.s.

[1] g of dry matter/m²; [2] n.s.: $p > 0.05$; *: $p < 0.05$; **: $p < 0.01$; ***: $p < 0.001$. Means followed by the same letter were not significantly different at $P \leq 0.05$ according to the Fisher's least significant difference (LSD).

In the sampling conducted on January 23, 2023 (123 das), the four biofumigant species tested reached dry biomass production levels that did not differ significantly, either in total biomass or in its two components (root and aboveground). The values ranged from 837 g dry matter/m² for *B. carinata* to 715 g dry matter/m² for *S. alba*. Furthermore, in all species, it was clear that the aboveground biomass contributed more significantly to the total dry biomass, representing between 84% and 91% of the total, depending on the species.

Approximately two months after the first sampling, and following a period of intense frost, the comparative analysis between the species showed changes in their ability to produce and accumulate biomass, compared to what was observed in the January 23 sampling. In this second sampling, both the ADB and TDB produced by *B. juncea* were significantly higher than those produced by *S. alba*, with *B. carinata* and *R. sativus* falling in an intermediate position. This was a result of the minimal variations in biomass accumulation levels shown by *B. juncea* and *R. sativus* compared to the previous sampling, in contrast to the significant decrease experienced by *B. carinata* and *S. alba* (Table 3).

Consequently, although none of the four species appears to be well-adapted to producing and accumulating biomass during periods of low temperatures (frost), it is evident that *B. carinata* and *S. alba* are extremely sensitive to such conditions (Figure 1). This fact is crucial when determining the most appropriate timing for their incorporation into soil in regions where frosts occur.

The results obtained from the 2022 autumn sowing highlighted the need to adjust the sampling schedule for biomass determination in the 2023 autumn sowing (Figure 1). The first biomass sampling was moved forward to 73 das (December 11, 2023), while the second sampling remained at a similar date to the first cycle (around 120 das). This adjustment was based on the species' sensitivity to frost, aiming to assess their biomass production capacity in shorter cycles, concluding before the onset of the frost period. The decision was further supported by the noticeably higher initial growth rates of *R. sativus* and *S. alba*, as corroborated by their higher levels of PAR interception.

 doi:10.20944/preprints202411.0247.v1

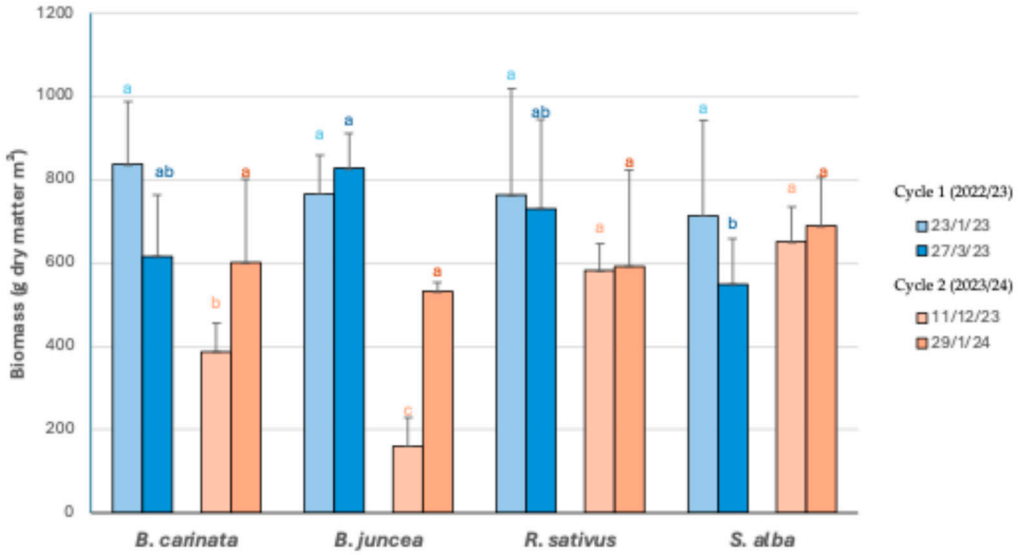

Figure 1. Comparative analysis of the Total Dry Biomass (TDB) produced by each biofumigant species in the two growing cycles and the two sampling dates. Means followed by the same letter were not significantly different at P ≤ 0.05 according to the Fisher's least significant difference (LSD).

In the sampling conducted on December 11, 2023 (73 das), in terms of TDB, the four species were grouped into three levels with statistically significant differences: the first group consisted of *S. alba* and *R. sativus*, which surpassed *B. carinata* in TDB, and the latter, in turn, produced and accumulated more biomass than *B. juncea.* These results confirm the higher capacity of *S. alba* and *R. sativus* to produce biomass in short cycles (around 70 das), compared to the potential shown by *B. carinata* and, especially, by *B. juncea* at that stage.

As for the analysis of the two components that determine TDB (ADB and RDB), the key difference is that *S. alba* accumulates more biomass in the ADB than *R. sativus*, while in the RDB, the situation is reversed.

By the end of January 2024, 48 days after the previous sampling (122 das), the four biofumigant species reached very similar TDB values, in line with the results observed in the equivalent sampling from the 2022 autumn sowing trial. This is because *R. sativus* and *S. alba* maintained similar production levels to the previous sampling, showing virtually no growth during that period. In contrast, *B. carinata* and, particularly, *B. juncea,* showed significant increases in TDB during that time, reaching levels comparable to the other two species (Figure 1). Regarding the analysis of the two components (ADB and RDB), the most noteworthy observation is the greater accumulation of root biomass (RDB) in *R. sativus* compared to the other three species.

Having conducted homologous samplings in both trial growing cycles (approximately 120 das) for biomass determination in the four biofumigant species, a statistical analysis was performed using the results from both growing cycles, confirming the findings identified in the individual analyses from each trial growing cycle (Table 4).

Table 4. Values and statistical analysis of Total Dry Biomass (TDB) and its components (Aboveground Dry Biomass - ADB and Root Dry Biomass - RDB) for the biofumigant species at 120 das, across both growing cycles.

Sources of variation	ADB[1]	RDB	TDB
B. carinata	639,8	79,2 b	719,0
B. juncea	513,1	136,6 ab	649,7
R. sativus	497,8	180,2 a	678,1
S. alba	626,1	75,6 b	701,7
Species	**ns[2]**	*	**ns**

 doi:10.20944/preprints202411.0247.v1

Cycle	*	n.s.	*
First	569,2 a[3]	117,9	687,1 a
Second	464,6 b	139,0	603,6 b
Species x cycle	**ns**	**ns**	**ns**

[1] g of dry matter/m²; [2] ns: p > 0.05; *: p < 0.05; **: p < 0.01; ***: p < 0.001. [3]Means followed by the same letter were not significantly different at P ≤ 0.05 according to the Fisher's least significant difference (LSD).

Although differences in biomass production were observed between the two growing cycles, particularly in terms of TDB, the general biomass distribution patterns remained consistent. *B. carinata* and *S. alba* showed a greater contribution of ADB to the TDB, while *R. sativus* stood out for its accumulation of root biomass RDB. Furthermore, the differences in production efficiency between the cycles reinforce the idea that climatic conditions and the duration of the cycle significantly influence the final performance of the biofumigant species. Nevertheless, the consistent behavior of the species in terms of biomass distribution suggests that management strategies, such as the timing of incorporation into the soil, should be adjusted according to these patterns. The results confirm that all species are capable of reaching similar levels of biomass accumulation, but with significant differences in how they allocate resources between the aboveground and root, which is a key factor to consider when implementing biofumigation strategies.

3.2. Radiation Interception and Radiation Use Efficiency

3.2.1. Fraction of Photosynthetically Active Radiation Intercepted by the Canopy (fIPAR)

The evolution of fIPAR by the different biofumigant species throughout the 2022-23 agronomic cycle undergoes significant variations (Figure 2).

The main differences in the evolution of fIPAR between the biofumigant species occurred in the initial and final stages of the 2022-23 cycle. In the initial stage (22 das), *R. sativus* and *S. alba* had higher fIPAR values than *B. carinata*, as a result of more vigorous early germination and growth. In turn, *B. carinata* showed higher fIPAR values than *B. juncea*.

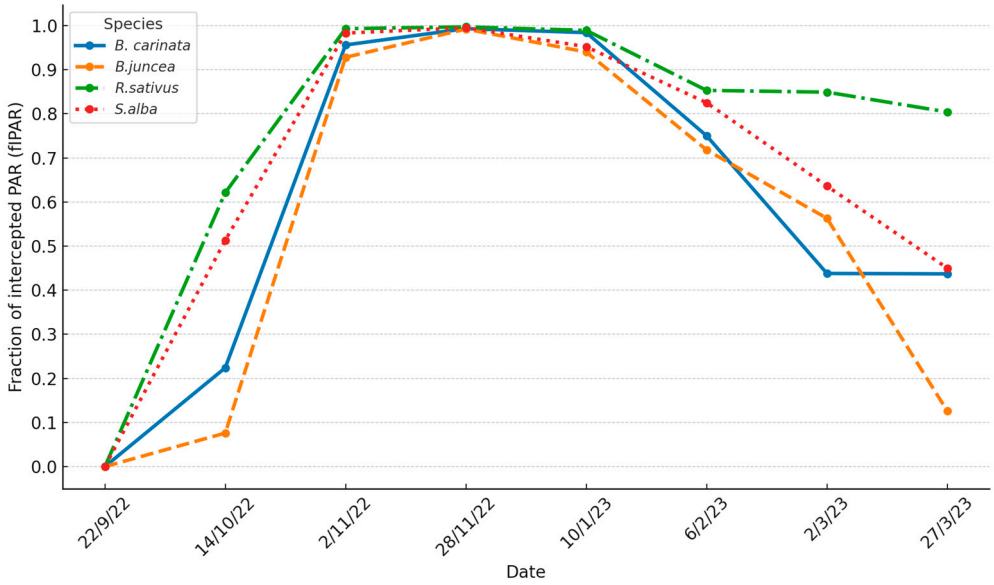

Figure 2. Evolution of the Fraction of Photosynthetically Active Radiation intercepted by the canopy (fIPAR) of the biofumigant species throughout the 2022-23 cycle.

As the cycle progressed, these initial differences between the species gradually decreased. By early November 2022 (41 das), only *B. juncea* showed lower PAR interception levels compared to the

 doi:10.20944/preprints202411.0247.v1

other species, which had already reached fIPAR values above 0.95. By the end of November 2022 (67 das) (Figure 2), fIPAR values approached 1 (between 0.99 and 1) in all four species.

Figure 3. Image of the biofumigant species trial on November 22, 2022 (67 das).

The frost period began in late November 2022 with three days of mild frost (minimum temperature ≥ -1.7º C). During December 2022 and the first half of January 2023, there were almost no frosts, and all four species continued to show very high fIPAR levels. However, in the last ten days of January 2023, much of February, and the first week of March 2023, the crop was subjected to a prolonged frost period (45 frost days, of which 25 days had minimum temperatures below -2º C, with some days reaching as low as -8º C).

As a result, by the end of January 2023, the species began to experience a decline in soil coverage or canopy shading, which was reflected in their fIPAR values. This decline was more pronounced in *B. carinata*, *B. juncea*, and *S. alba* compared to *R. sativus*. The process worsened in the following months, such that by early March, fIPAR values had dropped to around 0.5-0.6 for the first three species, while *R. sativus* maintained an fIPAR of around 0.85. This species was able to "renew and maintain" its canopy through continuous regrowth of the shoot, fueled by reserves stored in the root

3.2.2. PAR Intercepted During the Cycle and Radiation Use Efficiency

The integrated effect of the evolution of fIPAR was reflected in the total values of PAR intercepted by each of the biofumigant species from sowing until each of the two biomass sampling dates (123 and 186 das) (Figure 4).

 doi:10.20944/preprints202411.0247.v1

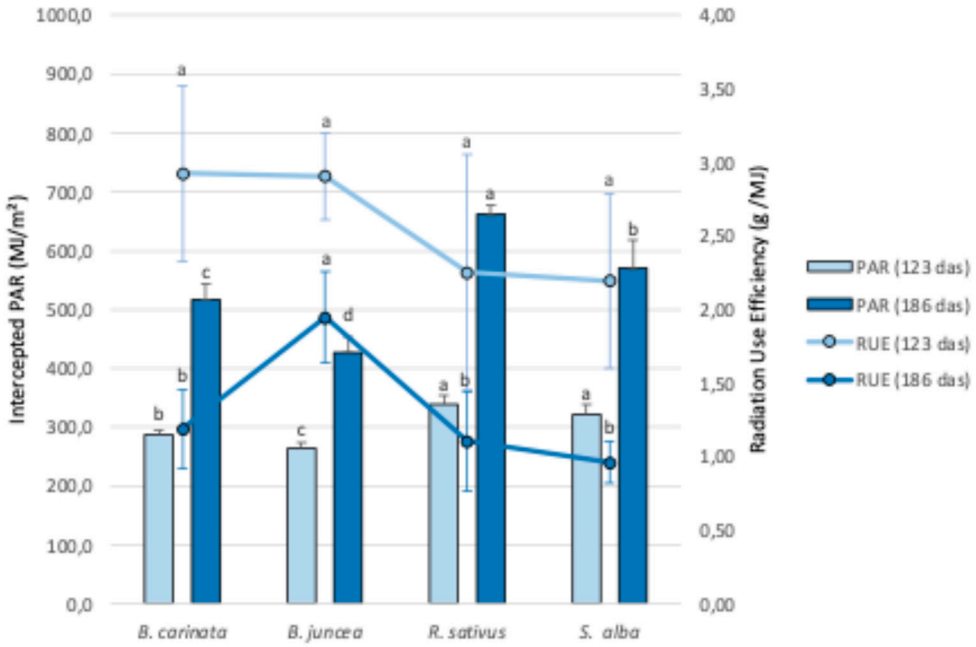

Figure 4. Intercepted PAR (MJ/m²), by the foliar cover on two dates (123 and 186 das), and PAR RUE, (g/MJ), of the biofumigant species during the entire cycle. Means followed by the same letter were not significantly different at P ≤ 0.05 according to the Fisher's least significant difference (LSD).

On the two analyzed dates, statistically significant differences were observed in the overall values of intercepted PAR between the species, with a similar general pattern in both cases. The RUE, a coefficient that indicates how the intercepted or absorbed PAR is used by the crop for biomass production, is known to vary based on multiple factors, including environmental stresses, phenological stages, genotypes [36], water and nitrogen availability [37], [2], species, crop management, weather conditions [38], and plant density [39], as well as the interactions between these factors [36]. *R. sativus* and *S. alba* intercept a greater amount of PAR due to faster initial growth and development compared to *B. carinata*, which in turn surpasses *B. juncea* in intercepted PAR. This is primarily the result of poorer and more irregular germination and slower initial growth in *B. juncea*. The only notable difference in the comparative analysis between species on both dates is that in the late March sampling (186 das), *R. sativus* intercepts more PAR than *S. alba*, as *R. sativus* was able to maintain a greater green foliar cover during the frost period.

Regarding the RUE values at 123 das, no statistically significant differences (5% significance level) were observed among the different biofumigant species, although both *R. sativus* and *S. alba* show slightly lower average values compared to the other two species. Therefore, there seems to be a clear compensatory effect between the two factors that determine biomass production (RUE and intercepted PAR), which explains why there are no statistically significant differences in accumulated biomass production up to that date among the four tested species. In line with previous studies, Brassica species tend to cover the soil rapidly, resulting in high radiation capture (517 MJ/m²), although their radiation use efficiency remains low (0.80 g/MJ) when compared to other cover crops [15].

Considering a cycle of 186 das, *B. juncea* reaches much higher RUE values compared to the other three species (Figure 4), with highly significant differences between the two groups. It is noteworthy that all four species show a decline in RUE due to greater foliar cover senescence, partly caused by the extended cycle through the end of winter and partly by the frost period they experienced during much of the winter. In any case, *B. juncea* exhibited the smallest decline in RUE. Once again, the integrated analysis of both parameters (intercepted PAR and RUE) perfectly explains the differences observed in biomass production among the different biofumigant species in the late winter sampling (186 das). *B. juncea* is the specie with the highest biomass production (with statistically significant differences compared to *S. alba*), as its lower capacity to intercept PAR—due to reduced growth under

 doi:10.20944/preprints202411.0247.v1

low-temperature conditions—is compensated by higher RUE values. In the case of *R. sativus*, the lower biomass production is attributed to its low RUE, not the amount of intercepted PAR. For the remaining two species (*B. carinata* and *S. alba*), the lower biomass accumulation is due to both a decrease in intercepted PAR and in RUE, which indicates that these two species are the most affected by low-temperature conditions in terms of biomass production and accumulation.

Furthermore, in the analysis of the correlations between accumulated biomass and the two factors that determine it (intercepted PAR and RUE), in both samplings (123 and 186 das), it is evident that the relationship between biomass and RUE is much stronger than that between biomass and intercepted PAR. This supports previous findings that show RUE as a more determinant factor for biomass production than PAR interception alone, particularly under varied environmental conditions and crop management approaches [36]. Ultimately, RUE better explains the biomass production capacity of the four tested biofumigant species than intercepted PAR (Figure 5).

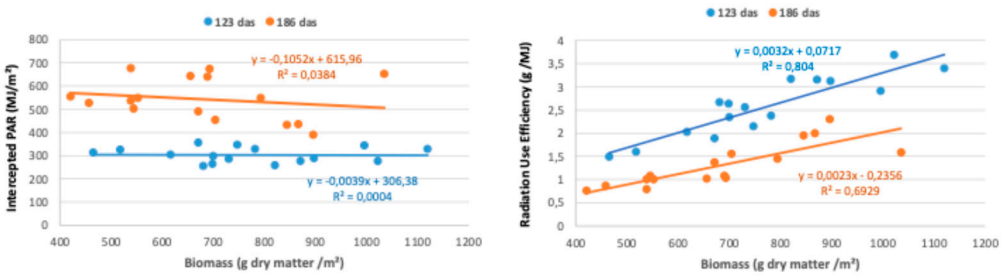

Figure 5. Analysis of the relationships between accumulated biomass at 123 and 186 days after sowing (das) and its determining components: intercepted PAR (left) and RUE (right).

3.3. Chlorophyll Content Index

In the first three SPAD measurement dates, corresponding to the period of the cycle during which frost had barely occurred (up until January 13, 2023), the statistical analysis of the results reveals that the four biofumigant species are grouped into two distinct categories with significant differences between them. The first group consists of *B. carinata* and *B. juncea*, with SPAD values ranging from approximately 37 to 39, while the second group includes *R. sativus* and *S. alba*, with SPAD values between approximately 30 and 33.

Table 5. Values and statistical analysis of the SPAD of biofumigant species on different sampling dates throughout the 2022-23 cycle.

Sampling date	***10-11-22***	***01-12-22***	***13-01-23***	***06-02-23***	***01-03-23***
B. carinata	36,9 a[1]	37,2 a	38,1 a	40,5 a	13,2 c
B. juncea	37,3 a	36,0 ab	38,9 a	37,4 ab	20,0 b
R. sativus	31,1 b	31,2 c	30,4 b	33,0 b	30,9 a
S. alba	33,6 ab	33,1 bc	32,9 b	25,2 c	12,7 c
p-value	*[2]	*	***	***	***

[2]n.s.: $p > 0,05$; *: $p < 0,05$; **: $p < 0,01$; ***: $p < 0,001$. [1]Means followed by the same letter were not significantly different at P ≤ 0.05 according to the Fisher's least significant difference (LSD).

In the data collection from early February 2023, the most notable difference compared to the previous observations is the significant decrease in the SPAD experienced by *S. alba*, which became statistically distinct from the SPAD values of *R. sativus*.

Finally, in early March 2023, after enduring a prolonged period of low temperatures, the differences in SPAD values among the biofumigant species became much more pronounced. This was due to the sharp decline in SPAD values observed in *B. carinata*, *B. juncea*, and *S. alba*, a trend not observed in *R. sativus*, which either maintained or only slightly decreased its SPAD values compared

 doi:10.20944/preprints202411.0247.v1

to previous measurements. As a result, at that time, the four biofumigant species grouped into three distinct levels with highly significant differences between them.

During the autumn of second sowing cycle (2023-2024), the SPAD was measured on January 29, 2024 (122 das). The results obtained on this date confirm a similar trend to that observed in the previous cycle (2022-23), both in the absolute SPAD values and in the significant differences among the biofumigant species.

In this cycle, *B. juncea* showed the highest SPAD values with a mean of 40.3 ± 2.6. These values are consistent with the results of the previous cycle, where *B. juncea* also exhibited high values, reflecting a strong ability to maintain elevated chlorophyll levels in its leaves. *B. carinata* also recorded a high SPAD values, with a mean of 38.7 ± 1.11, suggesting a consistent trend for this species regarding the SPAD parameter.

In contrast, *R. sativus* and *S. alba* displayed significantly lower SPAD values, with mean SPAD values consistently below 30. This difference between groups is in line with observations from the previous cycle, where both species also presented lower SPAD values compared to *B. carinata* and *B. juncea*.

These results reinforce the hypothesis that the SPAD index is strongly influenced by the biofumigant species, highlighting the importance of further investigating the relationship between this parameter and other key factors, such as the concentration of GLSs, which may contribute to the biofumigant potential of the species.

3.4. Glucosinolate Profiles and Isothiocyanate Potential

The GLSs profiles in the Brassica species analyzed during January and March of 2023 and 2024 showed a marked differentiation between aliphatic, aromatic, and indolic types, with significant variations in concentration among species (Figure 6). Specifically, *B. juncea* exhibited the highest overall GSLs concentration in both cycles and across months, with the values in January being notably higher than those in March. *S. alba* also presented high GSL levels, particularly in the second cycle's March sample, where it reached its peak concentration. In contrast, *B. carinata* and *R. sativus* demonstrated comparatively lower GSLs concentration, with *B. carinata* showing a substantial decrease from January to March, especially in the second cycle, suggesting seasonal or environmental influences on GSLs biosynthesis.

The Figure 6 illustrates these trends, where *B. juncea* and *S. alba* consistently dominate in GSLs levels, potentially highlighting their enhanced metabolic capacity for GSLs synthesis under varying conditions. The differences between cycles, represented by varying shades of blue, underscore potential annual environmental impacts or adaptations, as the second cycle showed slightly reduced concentrations for *B. juncea* in March, while *S. alba* reached its maximum in that period. These fluctuations point to species-specific responses to environmental variables, possibly due to differences in genetic regulation of GSLs pathways. The visual separation of values by month and cycle further emphasizes the importance of timing and environmental context in GSLs concentration and composition among *Brassica* species.

 doi:10.20944/preprints202411.0247.v1

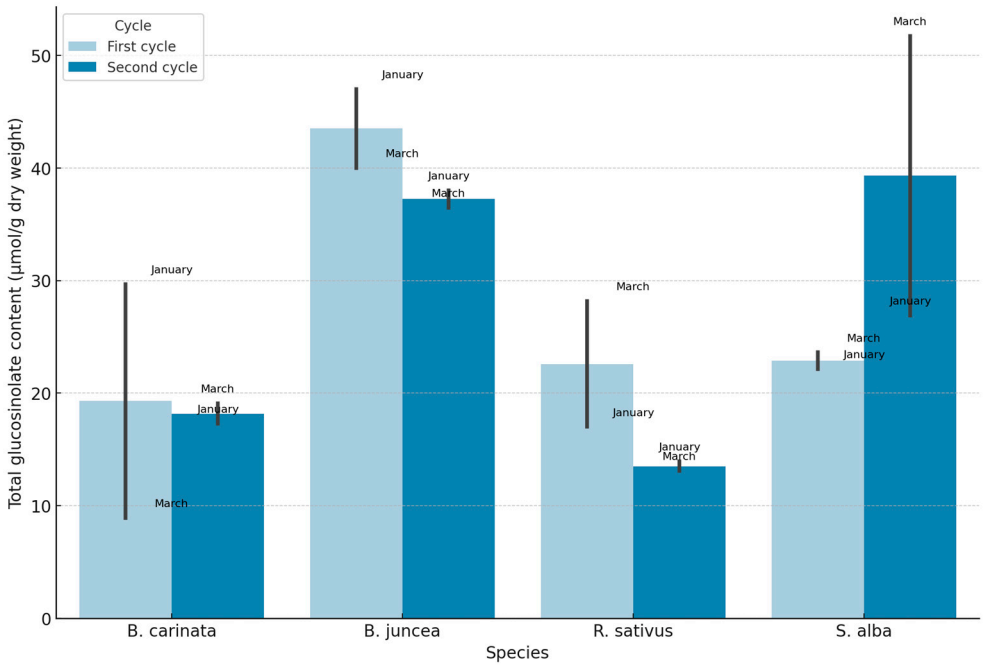

Figure 6. Total GSLs concentration in biofumigant plant species during first and seconc cycle (January and March sampling).

Aliphatic GSLs exhibited the highest concentrations in most species in both growing cycles, with Sinigrin standing out as a key compound in *B. juncea* and *B. carinata*, known for releasing ITC with fungicidal effects. Among these, Sinigrin was one of the most predominant aliphatic compounds, whose main product is allyl isothiocyanate, known for its bioactive properties. Other notable aliphatic GSLs included Glucoraphanin and Glucoerucin, which produce ITC such as sulforaphane and erucin, respectively, compounds with well-known effects on plant defense.

Additionally, Gluconapin and Glucotropaeolin contributed to the aliphatic profile in lower concentrations, with hydrolysis products such as benzyl isothiocyanate. Between January and March, aliphatic GSLs decreased by an average of 15-20% in these species, particularly in *B. juncea*, which could indicate an early defensive adjustment.

In contrast, the aromatic GSLs, primarily Sinalbin in *S. alba*, were more stable over the two growing cycles of analysis, showing a less seasonally dependent profile.

Regarding aromatic GSLs, Sinalbin and Gluconasturtiin were notable for their presence, with major products such as nitriles and phenethyl isothiocyanates. This stability in Sinalbin, which produces nitriles instead of ITC, may suggest a complementary defensive function, with fewer direct fungicidal effects. In *S. alba*, Sinalbin levels remained practically constant between January and March, suggesting a more consistent defensive role against other types of pathogens or environmental stress.

On the other hand, indolic GSLs, such as Glucobrassicin and 4-Hydroxyglucobrassicin, do not produce ITC, instead releasing hydrolysis products like indoles. These compounds serve critical defensive functions, possibly against herbivores or as signaling molecules in response to tissue damage, and do not provide direct fungicidal effects. In *R. sativus*, indolic GSLs were significantly concentrated in January, showing reductions of up to 25% by March. This could indicate a strategic defensive adaptation, with indolic compounds being preserved in early stages and reduced as the need for direct defense diminishes during the later growth phase.

Comparing species, *B. juncea* exhibited the most robust aliphatic GSLs profile, followed by *B. carinata*, suggesting its potential use in biofumigation strategies with stronger fungicidal effects. In *R. sativus*, the profile was more mixed, combining both aliphatic and indolic GSLs, which may not only provide an advantage in environments with a greater diversity of pathogens but also be of great importance as an alternative for rotating biofumigant species with different GSL profiles (Figure 7).

 doi:10.20944/preprints202411.0247.v1

Between the growing cycles, there was a trend of stability in aromatic GSLs and a slight reduction in aliphatic GSLs in 2024, particularly in March, suggesting an interannual adaptation in the defensive response of these species to environmental factors.

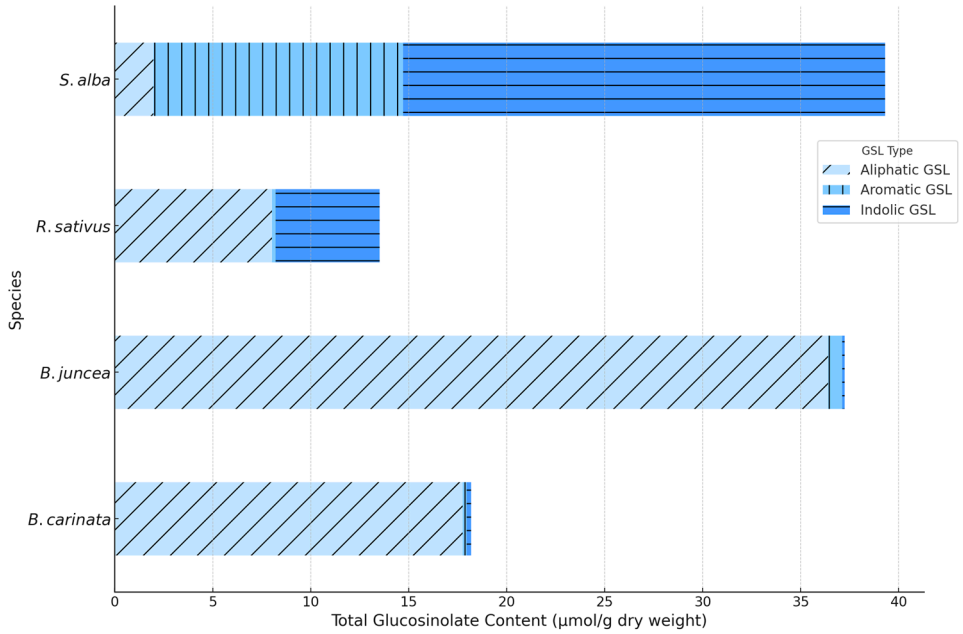

Figure 7. Comparison of aliphatic, aromatic, and indolic GSLs concentration in biofumigant plant species: 2023-2024.

These results *stress* the importance of considering both seasonal and interannual variations when developing Brassica-based biofumigation strategies, tailored to the specific challenges of each season and environment.

3.5. Correlation Analysis of Measured Variables

As highlighted in the previous section, the concentrations and profiles of GSLs show clear differences between the tested species, which indicates their likely differential biofumigant effect. These differences are much greater than those observed in the amounts of biomass produced by the species in 120-day cycles, suggesting that the differences in the total amounts of GSLs incorporated into the soil by the end of their cycle will largely depend on their GSLs concentration. The precise determination of these concentration and profiles requires labor-intensive sampling, treatment, and preservation procedures, as well as costly analytical determinations. Therefore, it is of great interest to analyze the potential relationships between crop indicators (biofumigant species) that are quick and easy to measure through proximal and/or remote sensors, and GSLs concentration, as a tool to assist decision-making regarding the optimal point in the cycle for incorporating biofumigant species biomass into the soil. One of these quick and easy-to-measure indicators is the SPAD index.

Figure 8 graphically shows the relationship between the total GSLs concentration in the biomass of the biofumigant species and the SPAD index from the samples taken in January and March 2023. In the January 2023 sampling, this relationship is consistent ($r^2 = 0.74$), exhibiting an exponential relationship: the higher the SPAD index, the higher the GSLs concentration.

In the March 2023 sampling, however, the relationship is much less consistent ($r^2 = 0.23$). It is very likely that the frosts occurring between the two samplings, which strongly affected the SPAD index of the species, were the most determining factor in the loss of consistency in this relationship.

Preprints.org (www.preprints.org) | NOT PEER-REVIEWED | Posted: 5 November 2024 doi:10.20944/preprints202411.0247.v1

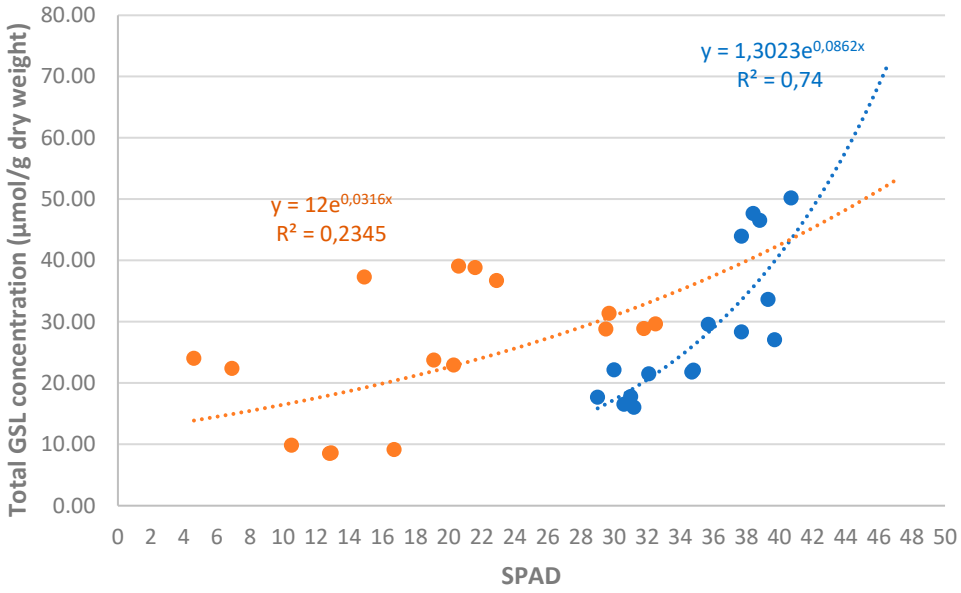

Figure 8. Individual analysis of the relationship between total GSL concentration in the biomass of biofumigant species and the SPAD values in the January (blue) and March (red) 2023 samplings.

As mentioned, SPAD values and GSLs concentration and profiles appear to be strongly dependent or linked to the species. However, many other environmental and agronomic management factors affect both parameters. In this regard, when analyzing results from multiple years, it is necessary to express the results in relative terms compared to a reference to eliminate the effect of additional sources of variation that may distort the analysis of this relationship. In this case, *B. juncea* was chosen as the reference species, as it showed the highest GSLs concentration and, along with *B. carinata*, was also among the species with the highest SPAD values.

The global analysis of this relationship, corresponding to the January 2023 and 2024 samplings (Figure 9), shows a very similar consistency ($r^2 = 0.71$) to that obtained in the individual analysis of January 2023 (Figure 8). This opens interesting possibilities for further investigation into this relationship and its consideration as a practical tool in the implementation of biofumigation strategies.

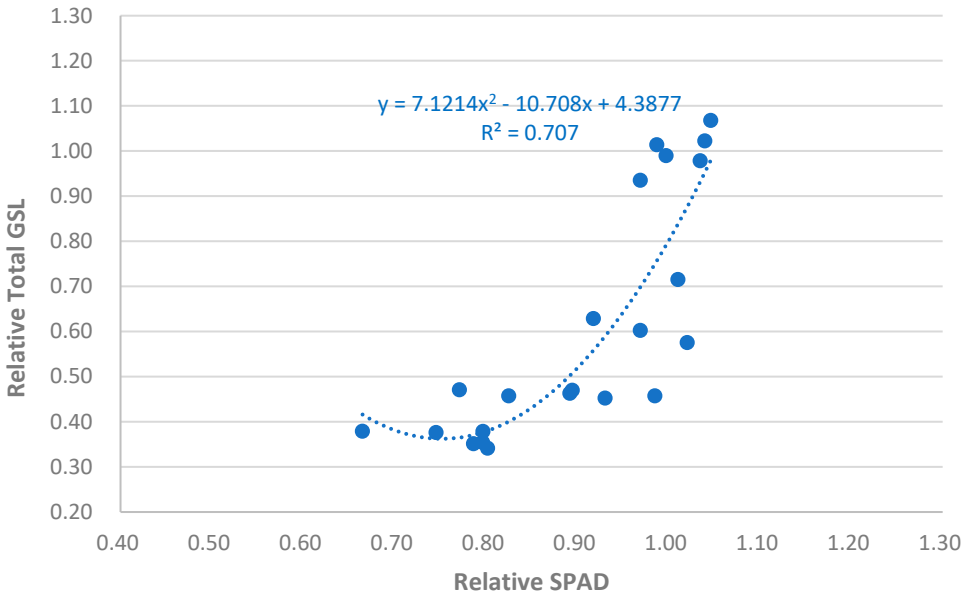

 doi:10.20944/preprints202411.0247.v1

Figure 9. Global analysis of the relationship between relative total GSLs concentration in the biomass of biofumigant species and the relative SPAD values in the January 2023 and 2024 samplings (120 das).

In summary, these results highlight the potential of using the SPAD values as an indirect estimator, at least in relative terms, of total GSLs concentration in the biomass of these four biofumigant species, serving as a tool to aid in the practical implementation of biofumigation. The need to use a reference species may present a "minor" practical inconvenience, but it is advisable whenever working with crop indicators, whose absolute values depend on many uncontrollable variables.

Additionally, these results also open the door to exploring other crop indicators of different types: chlorophyll-related indicators, such as Normalized Difference Red Edge (NDRE) index; vegetative development indicators, such as Normalized Difference Vegetation Index (NDVI) and Green Normalized Difference Vegetation (GNDVI); and combined indices such as Transformed Chlorophyll Absorption in Reflectance Index/ Optimized Soil-Adjusted Vegetation Index (TCARI/OSAVI), determined using remote sensors (multispectral cameras mounted on drones, satellite imagery). These indicators hold great potential for application on a larger scale (large plots) compared to the SPAD measurements obtained with portable reflectometers.

4. Discussion

While significant differences between the biofumigant species became evident in the second sampling date of the first cycle, particularly in aboveground biomass, the second cycle shows consistency in species with higher initial growth rates, such as *S. alba* and *R. sativus*. The aboveground biomass of *B. carinata* measured at mid-flowering stage, according to [35], ranged between 435–2417 g/m², with *S. alba* and *B. juncea* at 140–387 g/m² and 205–1792 g/m², respectively, reinforcing these species` significant biomass yield potential. These two species again outperformed *B. juncea* and *B. carinata* in biomass accumulation during the early samplings. This consistency across both cycles confirms that *S. alba* and *R. sativus* are more efficient at producing biomass in the early stages of cultivation, making them better suited for short cycles, such as those ending before frosts. Despite variation in biomass production, GSLs concentration within plant tissues is largely genetically determined but is also influenced by factors such as plant organs, developmental stage, and environmental conditions [17,28,35,40,41]. On the other hand, *B. juncea* and *B. carinata*, although initially showing slower growth, managed to catch up with the other species in the later stages of the cultivation cycle, suggesting a compensatory ability under more extended conditions.

Thus, the results from both cycles highlight the importance of tailoring the choice of biofumigant species to the duration of the cultivation cycle and specific climatic conditions, with particular attention to the sensitivity of some species to low temperatures. This selection process should also take into account biofumigant characteristics beyond GSLs concentration, such as biomass yield, adaptability to specific environmental conditions, and the species' ability to release bioactive compounds like ITC, as demonstrated in studies by [3].

The results of this study underscore the potential efficacy of Brassica species as biofumigants, particularly those with high levels of aliphatic GSLs, such as Sinigrin in *B. juncea* and *B. carinata*. According to [29], aliphatic GSLs are notably effective due to their ability to release volatile ITCs, which exhibit broad-spectrum toxicity against fungal pathogens and nematodes [29,35]. Our results show that aliphatic GSL concentrations were highest in these species during the January analysis, suggesting an adaptive strategy to maximize the release of bioactive compounds in the early growth stages. In fact, aliphatic GSLs such as sinigrin (0.1–26.5 and 10-20 µmol/g in *B. juncea* and *B. carinata*, respectively) were shown by [35] to dominate the aboveground biomass, contributing to their higher biofumigation efficacy [34,35].

Similarly, aromatic GSLs, such as Sinalbin in *S. alba*, showed less variability between sampling dates, which may reduce their efficacy compared to aliphatic ITCs for biofumigation, according to previous studies on ITC toxicity [29]. This behavior aligns with the stability of Sinalbin between

 doi:10.20944/preprints202411.0247.v1

January and March observed in our study, suggesting that aromatic GSLs may play a more constant defensive role against less volatile threats, such as insects [42]. However, aromatic GSLs, while highly toxic in controlled laboratory conditions [31], may be less effective in soil biofumigation due to their lower volatility and greater sorption to organic matter, reducing their diffusion in field settings [22,43].

Finally, although indolic GSLs, such as Glucobrassicin, do not produce ITCs, they may offer indirect benefits. Research by [35] indicates that indolic GSLs may induce defense responses in host plants, activating defense signals such as auxins and other related compounds [35]. This characteristic contributes to their lesser biofumigation potential but highlights their ecological role in plant defense. In our study, intermediate levels of indolic GSLs in *R. sativus*, particularly elevated in January, may indicate an early-stage adaptation to environmental conditions, potentially as a response to abiotic stress.

5. Conclusions

This comprehensive evaluation of Brassicaceae species for biofumigation reveals significant species-specific variations that are crucial for optimizing biofumigation strategies. Future research should focus on longitudinal studies to assess the impact of climatic variations on GSLs profiles and explore the genetic underpinnings of these traits to enhance biofumigant breeding programs. Overall, these findings suggest that the GSL profile and its seasonal variations can be optimized for biofumigation applications, and they highlight the potential of Brassica species for suppressing specific pathogens in crop rotation and management systems. Additionally, the possibility of using the SPAD index as an indirect indicator of GSL concentration for in-field decision-making should be further explored, as it could provide a practical tool for optimizing the timing of biomass incorporation in biofumigation practices.

Author Contributions: Conceptualization, J.A. and D.P.; methodology, J.A. and J.S; software, J.S.; validation, R.L. and Z.Z.; formal analysis, J.A. and D.P; investigation, J.A. and DP; resources, D.P.; data curation, J.A.; writing—original draft preparation, D.P and J.A.; writing—review and editing, R.L.; visualization, X.X.; supervision, J.A.; project administration, D.P.; funding acquisition, D.P. All authors have read and agreed to the published version of the manuscript.

Funding: This research was funded by Plan Estatal de Investigación Científica, Técnica y de Innovación 2021–2023 and Proyectos de Generación de Conocimiento, Convocatoria 2021 (PID2021-125545OR-C22).

Institutional Review Board Statement: Not applicable.

Conflicts of Interest: The authors declare no conflicts of interest.

References

1. Billen, G.; Aguilera, E.; Einarsson, R.; Garnier, J.; Gingrich, S.; Grizzetti, B.; Lassaletta, L.; Le Noë, J.; Sanz-Cobena, A. Beyond the Farm to Fork Strategy: Methodology for Designing a European Agro-Ecological Future. *Science of the Total Environment* **2024**, 908, 1–17. https://doi.org/10.1016/j.scitotenv.2023.168160.
2. Brennan, R. J. B.; Glaze-Corcoran, S.; Wick, R.; Hashemi, M. Biofumigation: An Alternative Strategy for the Control of Plant Parasitic Nematodes. *Journal of Integrative Agriculture*. Chinese Academy of Agricultural Sciences July 1, 2020, pp 1680–1690. https://doi.org/10.1016/S2095-3119(19)62817-0.
3. dos Santos, C. A.; de Souza, A. C.; Ferreira, M. G. Biofumigation with Species of the Brassicaceae Family: A Review. *Ciencia Rural* **2021**, 51 (1), 1–17. https://doi.org/http://doi.org/l0.1590/0103-8478cr2020040.
4. Kirkegaard, J. A.; Gardner, P. A.; Desmarchelier, J. M.; Angus, J. F. Biofumigation - Using Brassica Species to Control Pests and Diseases in Horticulture and Agriculture. In 9th *Australian Research Assembly on Brassicas*; Wratten, N., Mailer, R. J., Eds.; Agricultural Research Institute,: Wagga Wagga, 1993; pp 77–82.
5. Dutta, T. K.; Khan, M. R.; Phani, V. Plant-Parasitic Nematode Management via Biofumigation Using Brassica and Non-Brassica Plants: Current Status and Future Prospects. Current Plant Biology. Elsevier B.V. January 1, **2019**, pp 17–32. https://doi.org/10.1016/j.cpb.2019.02.001.
6. Karavina, C.; Mandumbu, R. Biofumigation for Crop Protection: Potential for Adoption in Zimbabwe. *J Anim Plant Sci* **2012**, 14 (3), 1996–2005.

7. Lazzeri, L.; Malaguti, L.; Cinti, S.; Ugolini, L.; De Nicola, G. R.; Bagatta, M.; Casadei, N.; D'Avino, L.; Matteo, R.; Patalano, G. The Brassicaceae Biofumigation System for Plant Cultivation and Defence. An Italian Twenty-Year Experience of Study and Application. *Acta Hortic* **2013**, 1005, 375–382. https://doi.org/10.17660/ActaHortic.2013.1005.44.
8. Ntalli, N.; Caboni, P. A Review of Isothiocyanates Biofumigation Activity on Plant Parasitic Nematodes. *Phytochemistry Reviews* **2017**, 16 (5), 827–834. https://doi.org/10.1007/s11101-017-9491-7.
9. Wei, F.; Passey, T.; Xu, X. Effects of Individual and Combined Use of Bio-Fumigation-Derived Products on the Viability of Verticillium Dahliae Microsclerotia in Soil. *Crop Protection* **2016**, 79, 170–176. https://doi.org/10.1016/j.cropro.2015.09.008.
10. Goswami, B.; Pariyar, B. Biofumigation-a Sustainable Alternative to Chemical Control of Soil Borne Pathogens: A Review. *International Journal of Advanced Multidisciplinary Research and Studies* **2024**, 4 (1), 134–138.
11. Gamliel, A.; van Bruggen, A. H. C. Maintaining Soil Health for Crop Production in Organic Greenhouses. *Sci Hortic* **2016**, 208, 120–130. https://doi.org/10.1016/j.scienta.2015.12.030.
12. Céspedes, C. L.; Avila, J. G.; Martínez, A.; Serrato, B.; Calderón-Mugica, J. C.; Salgado-Garciglia, R. Antifungal and Antibacterial Activities of Mexican Tarragon (Tagetes Lucida). *J Agric Food Chem* **2006**, 54 (10), 3521–3527. https://doi.org/10.1021/jf053071w.
13. Barros, A. F.; Campos, V. P.; da Silva, J. C. P.; Pedroso, M. P.; Medeiros, F. H. V.; Pozza, E. A.; Reale, A. L. Nematicidal Activity of Volatile Organic Compounds Emitted by Brassica Juncea, Azadirachta Indica, Canavalia Ensiformis, Mucuna Pruriens and Cajanus Cajan against Meloidogyne Incognita. *Applied Soil Ecology* **2014**, 80, 34–43. https://doi.org/10.1016/j.apsoil.2014.02.011.
14. Arnault, I.; Fleurance, C.; Vey, F.; Fretay, G. Du; Auger, J. Use of Alliaceae Residues to Control Soil-Borne Pathogens. *Ind Crops Prod* **2013**, 49, 265–272. https://doi.org/10.1016/j.indcrop.2013.05.007.
15. Elhakeem, A.; van der Werf, W.; Bastiaans, L. Radiation Interception and Radiation Use Efficiency in Mixtures of Winter Cover Crops. *Field Crops Res* **2021**, 264, 1–9. https://doi.org/10.1016/j.fcr.2020.108034.
16. Kalaji, H. M.; Dąbrowski, P.; Cetner, M. D.; Samborska, I. A.; Łukasik, I.; Brestic, M.; Zivcak, M.; Tomasz, H.; Mojski, J.; Kociel, H.; Panchal, B. M. A Comparison between Different Chlorophyll Content Meters under Nutrient Deficiency Conditions. *J Plant Nutr* **2017**, 40 (7), 1024–1034. https://doi.org/10.1080/01904167.2016.1263323.
17. Morris, E. K.; Fletcher, R.; Veresoglou, S. D. Effective Methods of Biofumigation: A Meta-Analysis. *Plant Soil* **2020**, 446 (1–2), 379–392. https://doi.org/10.1007/s11104-019-04352-y.
18. Matthiessen, J.; Kirkegaard, J. Biofumigation and Enhanced Biodegradation: Opportunity and Challenge in Soilborne Pest and Disease Management. *CRC Crit Rev Plant Sci* **2006**, 25 (3), 235–265. https://doi.org/10.1080/07352680600611543.
19. Hanschen, F. S.; Winkelmann, T. Biofumigation for Fighting Replant Disease-a Review. *Agronomy* **2020**, 10 (3), 1–16. https://doi.org/10.3390/agronomy10030425.
20. Kirkegaard, J. Biofumigation for Plant Disease Control – from the Fundamentals to the Farming System. In *Disease Control in Crops: Biological and Environmentally Friendly Approaches*; Walters, D., Ed.; Wiley-Blackwell,: Oxford, 2009; pp 172–195.
21. Fahey, J. W.; Zalcmann, A. T.; Talalay, P. The Chemical Diversity and Distribution of Glucosinolates and Isothiocyanates among Plants. *Phytochemistry* **2001**, 56, 5–51.
22. Clarkson, J.; Michel, V.; Neilson, R. Biofumigation for the Control of Soil-Borne Diseases. Soil borne disease focus group 2015. https://ec.europa.eu/eip/agriculture/sites/default/files/9_eip_sbd_mp_biofumigation_final_0.pdf (accessed 2024-11-01).
23. Agerbirk, N.; Olsen, C. E. Glucosinolate Structures in Evolution. *Phytochemistry* **2012**, 77, 16–45. https://doi.org/10.1016/j.phytochem.2012.02.005.
24. Gimsing, A. L.; Kirkegaard, J. A. Glucosinolates and Biofumigation: Fate of Glucosinolates and Their Hydrolysis Products in Soil. *Phytochemistry Reviews* **2009**, 8 (1), 299–310. https://doi.org/10.1007/s11101-008-9105-5.
25. Rosa, E. A. S.; Heaney, R. K.; Fenwick, G. R.; Portas, C. A. M. Glucosinolate in Crop Plants. In *Horticultural Reviews*; Janick, J., Ed.; Wiley, 1997; Vol. 19, pp 99–215.
26. Björkman, M.; Klingen, I.; Birch, A. N. E.; Bones, A. M.; Bruce, T. J. A.; Johansen, T. J.; Meadow, R.; Mølmann, J.; Seljåsen, R.; Smart, L. E.; Stewart, D. Phytochemicals of Brassicaceae in Plant Protection and

 doi:10.20944/preprints202411.0247.v1

Human Health - Influences of Climate, Environment and Agronomic Practice. *Phytochemistry* **2011**, 72 (7), 538–556. https://doi.org/10.1016/j.phytochem.2011.01.014.

27. Bellostas, N.; Sørensen, J. C.; Sørensen, H. Profiling Glucosinolates in Vegetative and Reproductive Tissues of Four Brassica Species of the U-Triangle for Their Biofumigation Potential. *J Sci Food Agric* **2007**, 87 (8), 1586–1594. https://doi.org/10.1002/jsfa.2896.
28. Fourie, H.; Ahuja, P.; Lammers, J.; Daneel, M. Brassicacea-Based Management Strategies as an Alternative to Combat Nematode Pests: *A Synopsis. Crop Protection* **2016**, 80, 21–41. https://doi.org/10.1016/j.cropro.2015.10.026.
29. Sarwar, M.; Kirkegaard, J. A. Biofumigation Potential of Brassicas II. Effect of Environment and Ontogeny on Glucosinolate Production and Implications for Screening. *Plant Soil* **1998**, 201, 91–101.
30. Brown, P. D.; Morra, M. J.; McCaffrey, J. P.; Auld, D. L.; Williams III, L. Allelochemicals Produced during Glucosinolate Degradation in Soil. *J Chem Ecol* **1991**, 17, 2021–2034.
31. Neubauer, C.; Heitmann, B.; Müller, C. Biofumigation Potential of Brassicaceae Cultivars to Verticillium Dahliae. *Eur J Plant Pathol* **2014**, 140 (2), 341–352. https://doi.org/10.1007/s10658-014-0467-9.
32. Borek, V.; Elberson, L. R.; McCaffrey, J. P.; Morra, M. J. Toxicity of Isothiocyanates Produced by Glucosinolates in Brassicaceae Species to Black Vine Weevil Eggs. *J Agric Food Chem* **1998**, 46, 5318–5323.
33. Morra, M. J.; Kirkegaard, J. A. Isothiocyanate Release from Soil-Incorporated Brassica Tissues. *Soil Biol Biochem* **2002**, 34, 1683–1690.
34. Bellostas, N.; Sørensen, J. C.; Sørensen, H. Qualitative and Quantitative Evaluation of Glucosinolates in Cruciferous Plants during Their Life Cycles. *Agroindustria* **2004**, 3 (3), 5–10.
35. Kirkegaard, J. A.; Sarwar, M. Biofumigation Potential of Brassicas I. Variation in Glucosinolate Profiles of Diverse Field-Grown Brassicas. *Plant Soil* **1998**, 201, 71–89.
36. Lake, L.; Sadras, V. O. Associations between Yield, Intercepted Radiation and Radiation Use Efficiency in Chickpea. In *18th Australian Society of Agronomy Conference*; RD Armstrong and L Hafner, Ed.; Australian Society of Agronomy: Ballarat, 2017; pp 24–28.
37. Wang, S.; Wang, E.; Wang, F.; Tang, L. Phenological Development and Grain Yield of Canola as Affected by Sowing Date and Climate Variation in the Yangtze River Basin of China. *Crop Pasture Sci* **2012**, 63 (5), 478–488. https://doi.org/10.1071/CP11332.
38. Manevski, K.; Lærke, P. E.; Jiao, X.; Santhome, S.; Jørgensen, U. Biomass Productivity and Radiation Utilisation of Innovative Cropping Systems for Biorefinery. *Agric For Meteorol* **2017**, 233, 250–264. https://doi.org/10.1016/j.agrformet.2016.11.245.
39. Morrison, M. J.; Stewart, D. W. Radiation-Use Efficiency in Summer Rape. *Agron J* **1995**, 87 (6), 1139–1142.
40. Larkin, R. P.; Griffin, T. S. Control of Soilborne Potato Diseases Using Brassica Green Manures. *Crop Protection* **2007**, 26 (7), 1067–1077. https://doi.org/10.1016/j.cropro.2006.10.004.
41. Winde, I.; Wittstock, U. Insect Herbivore Counteradaptations to the Plant Glucosinolate-Myrosinase System. *Phytochemistry* **2011**, 72 (13), 1566–1575. https://doi.org/10.1016/j.phytochem.2011.01.016.
42. Ashiq, S.; Edwards, S.; Watson, A.; Blundell, E.; Back, M. Antifungal Effect of Brassica Tissues on the Mycotoxigenic Cereal Pathogen Fusarium Graminearum. *Antibiotics* **2022**, 11 (9), 1–13. https://doi.org/10.3390/antibiotics11091249.
43. Ríos, P.; Obregón, S.; González, M.; de Haro, A.; Sánchez, M. E. Screening Brassicaceous Plants as Biofumigants for Management of Phytophthora Cinnamomi Oak Disease. *For Pathol* **2016**, 46 (6), 652–659. https://doi.org/10.1111/efp.12287.
44. Lazzeri, L.; Malaguti, L.; Cinti, S.; Ugolini, L.; De Nicola, G. R.; Bagatta, M.; Casadei, N.; D'Avino, L.; Matteo, R.; Patalano, G. The Brassicaceae Biofumigation System for Plant Cultivation and Defence. An Italian Twenty-Year Experience of Study and Application. Acta Hortic 2013, 1005, 375–382. https://doi.org/10.17660/ActaHortic.2013.1005.44.
45. Wang, S.; Wang, E.; Wang, F.; Tang, L. Phenological Development and Grain Yield of Canola as Affected by Sowing Date and Climate Variation in the Yangtze River Basin of China. Crop Pasture Sci 2012, 63 (5), 478–488. https://doi.org/10.1071/CP11332.